# Influences of Stiffness Ratio, Friction Coefficient and Strength Ratio on the Macro Behavior of Cemented Sand Based on DEM

**H. Zhao, Y. Sang, A. Deng and L. Ge**

**Abstract** A study was conducted on cemented sand modeled with a contact bond model to investigate the influences of micro parameters on its macro properties based on a three dimensional discrete element simulation. The influences of the micro parameters of the stiffness ratio, the strength ratio and the friction coefficient on the unconfined compression behavior of the cemented sand are revealed and a qualitative relationship is established between each individual micro parameter and the macro properties of Young's modulus and compressive strength based on 3D numerical discrete element simulation data. The results are important for the multi-scale study and will offer guidance to use the discrete element method, to model cemented sands or cemented aggregates.

## 1 Introduction

Natural soils are often characterized by a bonded structure such as carbonated sand [1]. Artificially treated sand by cement or chemical agents in ground improvement was widely applied in construction projects. Cemented sand are characterized by stiffening at low pressure and then yielding similar as over consolidated soils [1, 2], enhanced strength, a more brittle stress-strain response and a dilative volumetric behavior [3–5].

H. Zhao (✉)
State Key Laboratory of Structural Analysis for Industrial Equipment, Dalian University of Technology, Dalian 116023, China
e-mail: zhaoh@dlut.edu.cn

Y. Sang
Key Laboratory for Precision and Non-traditional Machining Technology of Ministry of Education, Dalian University of Technology, Dalian 116023, China

A. Deng
School of Civil, Environmental and Mining Engineering, The University of Adelaide, Adelaide, SA 5000, Australia

L. Ge
Department of Civil Engineering, National Taiwan University, Taipei 10167, Taiwan



X. Li et al. (eds.), *Proceedings of the 7th International Conference on Discrete Element Methods*, Springer Proceedings in Physics 188,
DOI 10.1007/978-981-10-1926-5_51

Since Cundall and Strack first developed the discrete element method (DEM) [6], it presents an effective method to investigate the global mechanical behavior and associated micro mechanisms occurring in granular materials. This method has been applied to model the cemented sand. Jiang et al. (2011) modelled shear behavior and strain localization in cemented sands by two-dimensional discrete element method based on contact bond model and then further developed a three dimensional contact bond model including rotation coefficient [7, 8]. Bono et al. applied the discrete element method to simulate the triaxial tests and one-dimensional compression of cemented sand consisting of crushable particles [9, 10].

In a DEM model, the mechanical properties of a specimen such as strength and moduli depend on the micro parameters defined at the particle level. Therefore it is very important to study the relations between the micro parameters of granular materials and their macro properties. These relations reflect the linkage of the behavior for granular materials at different scales and are important for the study of multi-scale problems. Previously, some work has been done to investigate the relationships between the micro parameters and macro properties. The effective moduli of regular packing of spheres are studied using Hertz-Mindlin contact model [11–13]. Potyondy and Cundall discussed the influences of several micro parameters on the macro behavior of rock base on a parallel bond model [14]. Plassiard et al. investigated the role of local parameters on the macro response via a parametric study and presented a calibration procedure for a DEM model using spherical elements with a local rolling resistance [15]. Dobry and Ng, Huang, Yang et al., and Ding et al. used the numerical simulations to investigate the micro-macro behavior of materials [16–19].

From the reviewed literatures, there are already a plenty of studies on the micro-macro relations for the granular materials. However, investigations on this relation for the cemented sand are scarce. Specially, it needs to establish a more qualitative relationship to link the macro parameters of the micro model to their macro properties, especially for the three dimensional specimens, which is more close to the real. Hence, the purpose of this paper is to investigate the influences of micro parameter on the stress-strain and macro properties for cemented sand based on the contact bond model with three dimensional DEM simulation of unconfined compression test. The contact bond model is selected because it can simulate the behavior of the cemented sand very well as illustrated by Jiang et al. and also has less micro parameters [7]. This work is performed with unconfined compressions tests by DEM simulation using PFC3D software.

## 2 Micro Parameters of a Contact Bond Model

A contact bond has the normal and shear strength $R_n$ and $R_t$ (in the unit of force) between two particles. When the corresponding component of the contact force exceeds either of these values, the bond breaks and the particle-particle behavior

reverts to that of an unbounded (granular) material. The contact bond can only transmit a force [20].

The main mechanical features of the contact bond model are shown in terms of the normal and tangential relative displacements versus the respective contact forces, $F_n$ and $F_s$. The relationship between force and displacements is linear until the bond breaks. The shear strength of the model is pressure independent at low stresses when the normal bond does not break while it increases linearly with the normal pressure at high normal stress when the normal bond breaks. This bond strength can be assumed to be provided by a purely cohesive contribution when the tangential contact force $F_s$ acting on the bond is low ($F_s < R_t/\tan\varphi_\mu$), and a purely frictional one when the shear force is high ($F_s > R_t/\tan\varphi_\mu$).The shear force is computed in an incremental form. The equations for the computation of contact forces are as following:

$$F_n = K_n U_n,\ F_n \leq R_n \tag{1}$$

$$\Delta F_s = -K_s \Delta U_s \tag{2}$$

$$K_n = \frac{k_n^A k_n^B}{k_n^A + k_n^B} = \frac{k_n}{2}\ K_s = \frac{k_s^A k_s^B}{k_s^A + k_s^B} = \frac{k_s}{2} \tag{3}$$

$$k_n = 4E_c R_0 \tag{4}$$

where $K_n$ and $K_s$ are the contact stiffness of two particles; $k_n^A, k_n^B, k_s^A, k_s^B$ are the particle normal stiffness and shear stiffness for ball A and ball B in contact; both have the same value of $k_n$ and $k_s$; $U_n$ is the overlap of two contacting particles; $\mu = \tan\varphi_\mu$, the friction coefficient; $E_c$ is the particle's elastic modulus; $R_0$ is the average radius of the two contacting particles. The failure criterion for the contact-bond model is:

$$\mathrm{F_n} = \mathrm{R_n};\ \mathrm{F_s} = \begin{cases} \mathrm{R_t} & \text{if } \mu \mathrm{F_n} \leq \mathrm{R_t} \\ \mu \mathrm{F_n} & \text{if } \mu \mathrm{F_n} > \mathrm{R_t} \end{cases}; \tag{5}$$

where $\mathrm{R_n}$ is the normal bond strength;$\mathrm{R_t}$ is the tangential bond strength; $\mathrm{F_n}$ is the normal acting force; $\mathrm{F_s}$ is the tangential acting force; μ is the interparticle friction coefficient.

Therefore, the item that characterizes the contact bond model is the grain and cement micro properties: $E_c$, $K_s/K_n$, $\mu$ and $R_n$, $R_t$. $E_c$ is the Young's moduli of the particle grain. In this study, three micro parameters are investigated: $K_s/K_n$, $\mu$, and $R_t/R_n$.

## 3 Macro Properties of UCT Specimens and DEM Simulation

Unconfined compression test (UCT) is commonly used to calibrate the micro parameters of the constitutive models in DEM in simulation of many different materials [21, 22]. Two major macro properties of elastic modulus $E$ and unconfined compressive strength $q_u$ are selected to study the influences of the selected micro parameters.

The numerical specimen is 100 mm in diameter and 200 mm in height. The total number of particles employed in each numerical specimen was around 25, 000. The average particle diameter is 0.002 m to minimize the particle size effects. The maximum to minimum radius ratio is 1.5. The specimens were generated with the radius expansion method. After the specimen was initially generated, the samples are running a number of cycles to reach the equilibrium state (unbalanced force becomes zero). A floater elimination procedure in the PFC3D User's Guide was then conducted to eliminate the unstable particles within the specimen. Finally, the contact bond is installed in the model. The cylindrical sidewall was then removed and the sample was ready to be loaded. The top and bottom walls act as loading platens. The specimen was loaded by moving the top and bottom walls towards each other at a specified velocity that ensures a quasi-static loading condition. Referring to the previous loading rate adopted, a loading rate of 0.002 m/s was selected for this study.

## 4 Effects of Contact Stiffness Ratio $K_s/K_n$

Numerous studies have been conducted on the contact stiffness ratio between solid objects. It is revealed that $K_s/K_n$, designated as $\eta_k$, is only dependent on the Poisson ratio of contacting materials for contacting rough surfaces. For the two bodies in contact made by the same material,

$$K_s/K_n = \chi\,\phi(v) \tag{6}$$

where $0.5 \le \chi \le 2$ is a constant and $\phi(\nu)$ is a function of the Poisson ratio $\nu$ of contacting particles.

Krolikowski and Szczepek (1993) also tested the tangential and normal stiffness of contact between rough surfaces using ultrasonic method for the fused quartz samples, the ratio of shear stiffness to normal stiffness $\eta_k = 0.94 \pm 0.11$ [23]. Gonzalez-Valadez et al. found for higher values of roughness, $\eta_k$ has a larger mean value, $\eta_k = 0.66 - 0.44$ for smooth sample, 0.48 – 0.68 for rough sample, 0.41 – 0.68 for rough sample with larger roughness values [24].

Even though there have been a few simulations done based on the discrete element method none of these studies discuss the influences of $\eta_k$ and the values

chosen were rather empirical. Based on the previously research findings, it is reasonable to assume $\eta_k$ is greater than 0.4 and less than 1.2 for the cemented sand.

To investigate the effects of $\eta_k$ on the behavior of the cemented granular materials, $\eta_k$ = 0.4, 0.6, 0.8, 1.0, 1.2 were selected. The value of $K_n$ is keeping a constant value of $1.0e^6$ N/m. The ratio of $\eta_k$ is changed by varying $K_s$ only. Other parameters used were $R_n = R_t = 50$ N, $\mu = 0.5$. The generated standard specimen is used in the simulation. The force chains of failed specimens are shown in Fig. 1. With different $\eta_k$, specimens fail in different deformation mode. With $\eta_k$ = 0.4, 0.6, the specimens failed by breakage of bonds at the top and bottom corner of the specimen. While with $\eta_k$ = 0.8, 1.0, 1.2, the specimens fail either by a shear band at the lower half of the specimen or by bond breakage at the top and bottom end, which are more close to real failure observations. Therefore, it is reasonable to assume that $\eta_k$ should be greater than 0.6 in the simulation of cemented sand with an appropriate bond value.

The stress-strain curves for the specimens are illustrated in Fig. 2, which show a brittle failure pattern and the failure strain is small. The normalized elastic moduli $(E/E_{\_\eta_k=1.0})$ and the normalized unconfined compressive strength $q_u/q_{u\_\eta_k=1.0}$ versus stiffness ratio $\eta_k$ are plotted in Fig. 3. The obtained normalized elastic moduli are decreasing with the increase of $\eta_k$ and the normalized compressive strengths are increasing with $\eta_k$. However, when $\eta_k$ is greater than 1.0, both stop increasing.

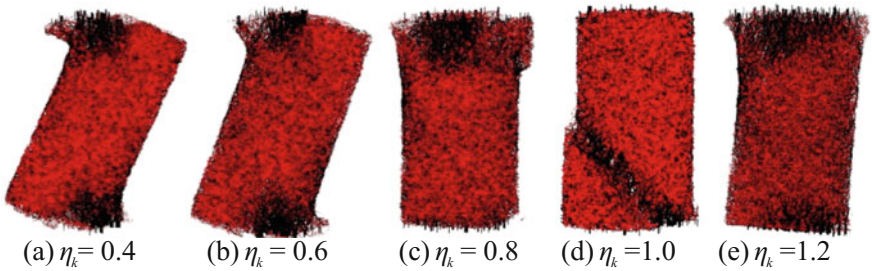


**Fig. 1** The force chains of failed specimens in UCT test

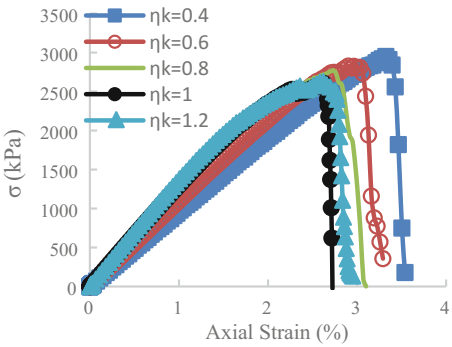


**Fig. 2** Stress-strain *curves* with different $\eta_k$

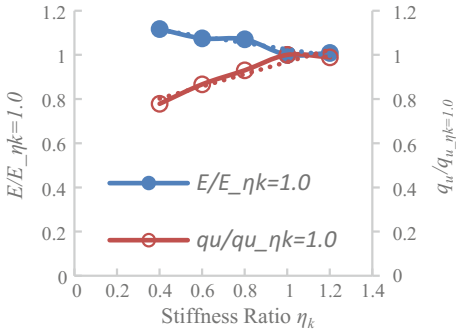


**Fig. 3** $E/E_{\_\eta_k=1.0}$ and $q_u/q_{u\_\eta_k=1.0}$ versus $\eta_k$


**Fig. 4** The force chains of the failed specimens in UCT test, $\mu$ = 0.2, 0.5; 0.75, 1.0, 1.2

## 5 Effects of Friction Coefficient $\mu$

Intergranular friction coefficient $\mu$ reflected the intergranular friction angle $\varphi_\mu$, $\mu = \tan\varphi_\mu$. Since the friction angle for sand is usually less than 50°, $\mu$ should be less than 1.25. The friction coefficient $\mu$ with the value of 0.25, 0.5, 0.75, 1.0, and 1.25 are selected to study their influences on the macro properties of the cemented sand based on the DEM simulation of the contact bond model. Other parameters selected are $K_n = K_s = 1e^6$ N/m; $R_t = R_n = 50$ N. The force chains for the failed specimens are shown in Fig. 4. It is clear that $\mu$ has an influence on the unconfined compression failure behavior of the cemented sand. Except for $\mu$ = 0.25 and 0.5, the other specimens all failed by forming a fully developed shear band at the lower half of the specimen. When $\mu$ = 0.25 and 0.5, there are localized failure at the top and bottom of the specimen.

The obtained stress-strain curves for the tested specimens are shown in Fig. 5. It was found when μ is less than 0.5, it has a significant influence on the peak stress and the strain developed; when μ is greater than 0.5, its influence is very small. The normalized elastic modulus $E_{nor}$ ($E/E_{\_\mu=1.0}$) and the normalized unconfined compressive strength $q_{u\_nor}$ ($q_u/q_{u\_\mu=1.0}$) are plotted in Fig. 6. The normalized elastic modulus is not affected by the friction coefficient. The normalized strength is increasing with $\mu$ when $\mu$ is less than 0.8 and becomes constant afterwards. These

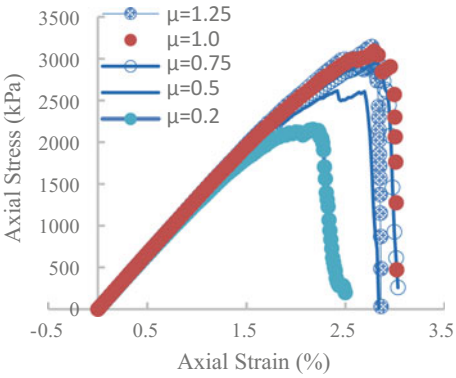


**Fig. 5** Stress-strain *curves* with different $\mu$

results indicate that $\mu$ has rather limited influences on the macro properties of the cemented sand.

## 6 Effects of Bond Strength Ratio

The failure of the cemented sand is controlled by the cementation strength between the sand particles due to the hydrated cement. The distribution of hydrated cement is affected by many factors such as the thickness of the cementation, the hydration degree, the water cement ratio, the hydration products etc. The cementation strength is reflected by the strength parameters of $R_t$ and $R_n$ in the contact bond model for the DEM simulation. Hence it is important to investigate the influence of these strength parameters on the macro properties of the cemented sand to guide the selection of the appropriate values of $R_t$ and $R_n$. The investigation is conducted through studying the influences of the ratio of $R_t/R_n$ on the macro properties of the specimens. By varying $R_t$ values and keeping $R_n$ constant, a series of UCT simulations were conducted with different $R_t/R_n$ values of 0.25, 0.5, 0.75, 1.0, 1.5, 5.0, 10.0, 100. This large range of $R_t/R_n$ is selected because the cementation distribution is very random. The other parameters for the specimens are $K_n = K_s = 1e^6$ N/m, $R_n = 50$ N, $\mu = 0.5$. The distributions of the force chains for the failed specimens are shown in Fig. 7. When $R_t/R_n$ is not greater than 1, the specimens either fail by a large compression deformation or by developing a complete shear band; However, when $R_t/R_n$ is greater than 1, the specimens fail by localized shear band at the corners of top and bottom of the specimen or by developing a splitting failure pattern through the top to the bottom of the specimen.

The shear bond strength value $R_t$ of contact bonded model controls the behavior of the particles in the tangent direction. When the shear force reaches the shear bond strength, the bond is breaking in the tangent direction; the particles start to slide and behave simply as that of a contact model. When $R_t/R_n > 1$, the particles are not easy to break in the shear direction, thus the particles would tend to break in the normal

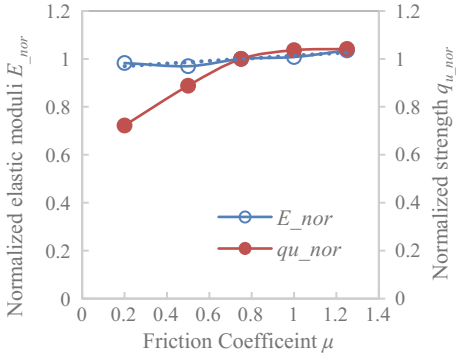


**Fig. 6** $E_{nor}$ and $q_{u\_nor}$ versus $\mu$

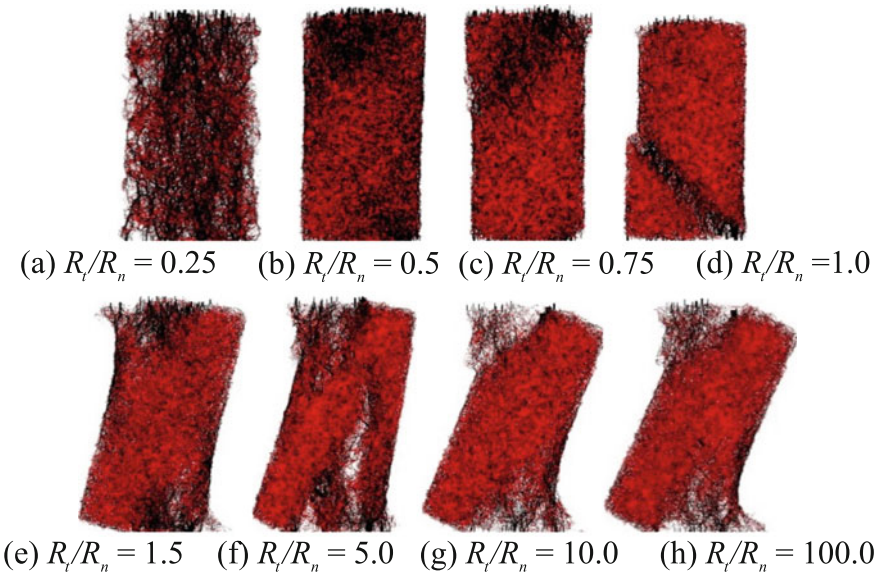


**Fig. 7** The force chains of failed specimens with different $R_t/R_n$

direction with a splitting failure pattern in the normal direction. Since the sand particles have high compressive strength, thus the unconfined compressive strength is also much higher with higher values of $R_t/R_n$. This explains the failure pattern observed in Fig. 7.

The stress-strain curves obtained from the numerical simulations are plotted in Fig. 8. When $R_t/R_n < 1.0$, the axial stress is increasing linearly and then reaches the yield stress, further nonlinearly increasing to a peak point and then becomes softened. While $R_t/R_n > 1.0$, the axial stress is linearly increasing and then drops suddenly.

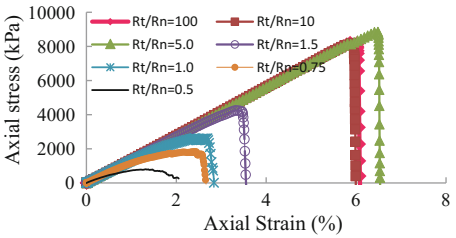


**Fig. 8** Stress-strain *curves* for UCT specimens with different strength ratios

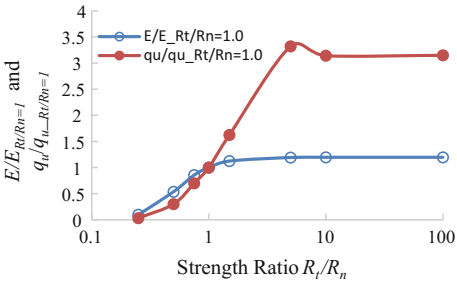


**Fig. 9** $E/E_{\_R_t/R_n=1.0}$ and $q_u/q_{u\_R_t/R_n=1}$ versus strength ratio $R_t/R_n$

The variation of obtained normalized strength $q_u/q_{u\_R_t/R_n=1}$ and the extracted normalized elastic modulus $E/E_{\_R_t/R_n=1.0}$ are plotted in Fig. 9 versus the strength ratio $R_t/R_n$. When $R_t/R_n > 1.5$, the normalized elastic modulus increases with $R_t/R_n$; When $R_t/R_n > 10$, the normalized elastic modulus keeps constant. This is possibly because the shear strength controls the failure of the specimen when shear strength is less than the normal strength. However, when $R_t$ is greater than $R_n$, the normal bond strength is controlling the behavior of the specimen; since $R_n$ is constant, the normalized elastic modulus therefore keeps constant. The strength and elastic modulus values increase first quickly with normal bond strength and then becomes almost constant. They also show a similar variation trend with bond shear strength. The normalized unconfined compressive strength is also increasing with the increasing of bond strength ratio when $R_t/R_n < 5.0$ and keeping constant when $R_t/R_n > 5.0$, which can be explained as that the specimen now fails in splitting mode with normal breakage of the contact bonds with a constant $R_n$ value in the simulations.

It is clear that the bond strength has a great influence on the behavior of contact bonded granular material from UCT simulations. The failure mode of the specimens depends on the ratio of the two strength values. When $R_t/R_n \leq 1$, the specimen fails in a shearing mode; When $R_t/R_n > 1$, the specimen fails in a splitting mode.

## 7 Conclusions

Investigations of micro parameters of contact bond model on the macro properties of simulation of cemented sand were conducted using DEM simulation of UCT. The study reveals that the micro parameters of $K_s/K_n$, $\mu$, strength ratio and $R_t/R_n$ have different influences on the macro behavior of cemented sand.

Stiffness ratio greater than 0.6 will promote a shear band failure in this study which is more close to the experimental observations on cemented sand. A range of 0.6 to 1.2 is recommended for simulation of cemented sand. The obtained normalized elastic moduli are decreasing with the increase of $\eta_k$ and the normalized compressive strengths are increasing with $\eta_k$. However, with $\eta_k$ greater than 1.0, both become constant.

The friction coefficient does not affect the normalized elastic moduli and the peak shear strength when it is greater than 0.5. Below 0.5, both elastic moduli and the peak shear strength would increase with the friction coefficient. The variation of $\mu$ does not cause much influence on the failure pattern except when $\mu$ is lower than 0.5. An upper bound value of 1.25 is proposed for the simulation of cemented sand considering its physical meaning.

The bond strength has a great influence on the behavior of contact bonded granular material from UCT simulations. The failure mode of the specimens depends on the ratio of the two bond strength values, the specimen fails in a shearing mode when $R_t/R_n \leq 1$ and in a splitting mode when $R_t/R_n > 1$, $E/E_{-R_t/R_n=1.0}$ increases with $R_t/R_n$ with $R_t/R_n < 1.5$ and keeps constant with $R_t/R_n > 1.5$.

**Acknowledgments** This research was supported by the National Natural Science Foundation of China (No. 51308091, No. 51275068), and supported by the Fundamental Research Funds for the Central Universities (DUT15QY48).

## References

1. Airey, D.W.: Triaxial testing of naturally cemented carbonate soil. J. Geotech Eng. **119**, 1379–1398 (1993). ASCE
2. Leroueil, S., Vaughan, P.R.: The general and congruent effects of structure in natural soils and weak rocks. Geotechnique **40**(3), 467–488 (1990)
3. Dupas, J., Pecker, A.: Static and dynamic properties of sand-cement. J. Geotech Eng. **105**, 419–436 (1979). ASCE
4. Acar, Y.B., El-Tahir, A.E.: Low strain dynamic properties of artificially cemented sand. J. Geotech. Eng. **112**, 1001–1015 (1986). ASCE
5. Clough, G.W., Sitar, N., Bachus, R.C., Rad, N.S.: Cemented sands under static loading. J. Geotech Eng. **107**, 799–817 (1981). ASCE
6. Cundall, P.A., Strack O.: A discrete numerical model for granular assemblies. Geotechnique **29**(1), 47–65 (1979)

7. Jiang, M.J., Yan, H.B., Zhu, H.H., Utli, S.: Modeling shear behavior and strain localization in cemented sands by two-dimensional distinct element method analyses. Comput. Geotech. **38** (1), 14–29 (2011)
8. Jiang, M., Shen, Z., Wang, J.: A novel three-dimensional contact model for granulates incorporating rolling and twisting resistances. Comput. Geotech. **65**, 147–163 (2015)
9. De Bono, J.P., Mcdowell, G.R.: Discrete element modeling of one-dimensional compression of cemented sand. Granul. Matter **16**(1), 79–80 (2014)
10. de Bono, J.P., McDowell, G.R., Wanatowski, D.: DEM of triaxial tests on crushable cemented sand. Granul. Matter **16**, 563–572 (2014)
11. Duffy, J., Mindlin, R.D.: Stress-strain relations and vibrations of a granular medium. J. Appl. Mech. **24**, 585–593 (1957). ASME
12. Deresiewicz, H.: Mechanics of granular matter. Adv. Appl. Mech. **5**, 233–306 (1958)
13. Walton, K.: The oblique compression of two elastic spheres. J. Mech. Phys. Solids **26**, 139–150 (1978)
14. Potyondy, D.O., Cundall, P.A.: A bonded-particle model for rock. Int. J. Rock Mech. Min. Sci. **41**, 1329–1364 (2004)
15. Plassiard, J.-P., Belheine, N., Donzé, F.-V.: A spherical discrete element model: calibration procedure and incremental response. Granul. Matter **11**(5), 293–306 (2009)
16. Dobry, R., Ng, T.-T.: Discrete modeling of stress-strain behavior of granular media at small and large strains. Eng. Comput. **9**, 129–143 (1992)
17. Huang, H.Y.: Discrete element modeling of tool-rock interaction. PhD thesis, University of Minnesota, Minneapolis (1999)
18. Yang, B., Jiao, Y., Lei, S.: A study on the effects of microparameters on macro-properties for specimens created by bonded particles. Eng. Comput. **23**(6), 607–631 (2006)
19. Ding, X., Zhang, L., Zhu, H., Zhang, Q.: Effect of model scale and particle size distribution on PFC3D simulation results. Rock Mech. Rock Eng. **47**, 2139–2156 (2014)
20. Itasca. PFC3D Particle Flow Code in 3 Dimensions User's Guide (2005)
21. Fakhimi, A., Villegas, T.: Application of dimensional analysis in calibration of a discrete element model for rock deformation and fracture. Rock Mech. Rock Eng. **40**(2), 193–211 (2007)
22. Hentz, S., Daudeville, L., Donze, F.V.: Discrete element modeling of a reinforced concrete structure. J. Mech. Behav. Mater. **19**(19), 245–258 (2009)
23. Krolikowski, J., Szczepek, J.: Assessment of tangential and normal stiffness of contact between rough surfaces using ultrasonic method. Wear **160**, 253–258 (1993)
24. Gonzalez-Valadez, M., Baltazar, A., Dwyer-Joyce, R.S.: Study of interfacial stiffness ratio of a rough surface in contact using a spring model. Wear **268**(3–4), 373–379 (2010)